Pavel A. Perezhogin*, Andrey V. Glazunov, and Andrey S. Gritsun

Stochastic and deterministic kinetic energy backscatter parameterizations for simulation of the two-dimensional turbulence

https://doi.org/10.1515/rnam-2019-0017
Received April 3, 2019; accepted May 21, 2019

Abstract: The problem of modelling 2D isotropic turbulence in a periodic rectangular domain excited by the forcing pattern of prescribed spatial scale is considered. This setting could be viewed as the simplest analogue of the large scale quasi-2D circulation of the ocean and the atmosphere. Since the direct numerical simulation (DNS) of this problem is usually not possible due to the high computational costs we explore several possibilities to construct coarse approximation models and corresponding subgrid closures (deterministic or stochastic). The necessity of subgrid closures is especially important when the forcing scale is close to the cutoff scale of the coarse model that leads to the significant weakening of the inverse energy cascade and large scale component of the system dynamics.
The construction of closures is based on the *a priori* analysis of the DNS solution and takes into account the form of a spatial approximation scheme used in a particular coarse model. We show that the statistics of a coarse model could be significantly improved provided a proper combination of deterministic and stochastic closures is used. As a result we are able to restore the shape of the energy spectra of the model. In addition the lagged auto correlations of the model solution as well as its sensitivity to external perturbations fit the characteristics of the DNS model much better.

Keywords: Two-dimensional turbulence, stochastic parameterization, kinetic energy backscatter, subgrid scale modelling, scale-similarity.

MSC 2010: 76F05, 76F65, 76M20, 76M35, 76M55

1 Introduction

Correct description of atmospheric and oceanic dynamics must take into account a huge range of interacting scales resulting in the fact that direct numerical simulation (DNS) of the global circulation is technically impossible. The traditional way to reduce computational costs is to follow large eddy simulation or LES [17] ideology where only the large scale component of the flow is modelled directly while unresolved small scales and corresponding resolved-unresolved scale interactions must be somehow parameterized. Modelling of unresolved scales and forces represent the so-called closure problem. In a 3D turbulence case there are several well known approaches to tackle this problem [50]. However, in a 2D case the LES approach is less studied. Moreover it must be different from the 3D one as the equations for the 2D turbulence have some specific properties. In particular, they allow one to specify the additional (to the 3D case) conservation laws, the so-called Casimir invariants [20, 21, 46–48, 51]. The second Casimir invariant (the enstrophy) plays especially important role for the 2D flows. It causes redistribution of the energy to the large scales in forced turbulence problem [11, 29]. It should be noted that due to the strong difference in vertical and horizontal scales, the large scale atmospheric and oceanic circulation could be viewed as a quasi-two-dimensional geophysical

***Corresponding author: Pavel A. Perezhogin,** Marchuk Institute of Numerical Mathematics of the Russian Academy of Sciences, Moscow 119333, Russia. E-mail: pperezhogin@gmail.com
Andrey V. Glazunov, Andrey S. Gritsun, Marchuk Institute of Numerical Mathematics of the Russian Academy of Sciences, Moscow 119333, Russia

turbulence [16]. That is why the LES approach in 2D case must be studied in more detail to provide physically consistent parameterizations for global general circulation models.

Additional aspect that should be taken into account while constructing subgrid parameterizations is a numerical scheme used for spatial approximation of model equations. Let us focus on the simplest mathematical model approximating to the first order dynamics of quasi 2D turbulent flows in atmosphere and ocean, namely the system of 2D incompressible fluid equations. According to the classical Kraichnan–Leith–Batchelor similarity theory (KLB, [7, 29, 33]) the energy from the forcing acting in a small spectral interval near some wavenumber k_f is transferred to the larger scales while the enstrophy redistributes to the smaller ones. As a result (in a non-dissipative case) two inertial intervals should emerge with the energy spectrum in the following form:

$$E(k) = \begin{cases} C_f \varepsilon^{2/3} k^{-5/3}, & k \leqslant k_f \\ C_b \eta^{2/3} k^{-3}, & k > k_f \,. \end{cases} \tag{1.1}$$

Here ε and η are the energy and enstrophy inflow per unit surface, respectively.

Similarity theory assumes spectrally local transfers of energy and enstrophy in inertial ranges. The nonlocal nonlinear interactions between scales with $k \leqslant k_f$ and $k > k_f$ lead to deviations of the spectra from the KLB theory predictions especially in the short-wave range where strain rate becomes nonlocally dominated [30]. The exact shape of the long-wave range energy spectrum is also debatable (see [9] and overview in this paper).

As was shown in [26] the spatial discretization of the model equations works effectively as an additional filtration of the small scales applied to the system dynamics. In some cases it could distort energy/enstrophy cascades in the model. When the turbulence is excited by a large scale forcing, system dynamics is mainly controlled by the prolonged direct enstrophy cascade and large scales are not sensitive to a spatial approximation applied. Conversely, in the case of a small scale forcing, numerical scheme errors distort and damp circulation on a forcing scales. As a result models usually have weakened backward energy cascade and significantly damped large scale circulation (some examples are presented below, see also [45]). The latter case is the most challenging one for constructing subgrid parameterizations. Note that the small scale forcing case is relevant to the problem of modelling general oceanic circulation as atmospheric winds and mesoscale eddies could be viewed as a small scale oceanic driver.

Currently there are several approaches to constructing subgrid scale parameterizations for 2D turbulence systems. The common basic principle is to reconstruct missing subgrid forces producing enough dissipation of the enstrophy and conservation (exact or approximate) of the energy in a system. One of the widely used ideas here is to restore somehow (unresolved) energy transfer from subgrid scales to the large ones (i.e., provide 'kinetic energy backscatter' or KEB [52]). These schemes could be further divided into two large groups of stochastic [8, 52] and deterministic parameterizations. In turns the deterministic KEB schemes could be linear [1, 27, 58] or nonlinear [10, 14, 49]. Techniques combining stochastic and deterministic approaches also exist [15, 23]. Usually the closure construction is based on the *a priori* analysis of the high resolution model (DNS) output to estimate statistics of correspondent subgrid forces. It is important to include into consideration an advection scheme of a coarse model [26, 53, 58].

Besides ideas relying on the energy redistribution approach one can also mention MTV (Majda–Timofeyev–Vanden Eijnden) or stochastic mode reduction method [36] based on the assumption of the time scale separation between the small and large scales. The MTV gives encouraging results for 1D systems like Burgers equation [18] and for 2D systems (barotropic vorticity equation on a sphere [22] with a small number of retained degrees of freedom). Though for the finite difference version of the 2D incompressible fluid this approach is yet to be developed. Also mention another approach to constructing subgrid parameterizations for systems with weak coupling that is based on the response theory and was proposed in [63] and [62].

Before describing the content of the work presented in the paper we would like to mention one important problem related to the use of subgrid parameterizations. For the climate modelling studies it would be very desirable to have reduced system approximating correctly not only statistics of the original model (nature) but its sensitivity to an external forcing. The second requirement does not follow from the first one [2] and is

very nontrivial. As a result we must check not only the basic statistical properties of reduced models (energy spectra etc.) but also their sensitivity properties.

In this paper we study the problem of modelling 2D incompressible fluid forced by a small scale forcing. We avoid the analysis of model dynamics in the enstrophy inertial range and focus on the ability of numerical model to predict the inverse energy cascade, even when the mesh cutoff is very close to the scale of external forcing. We restrict ourselves to the uniformly isotropic case keeping in mind the fact [10] that the closures obtained for this simple system could be generalized to the more general case with nonzero rotation. We consider four different numerical schemes for spatial approximation of the model equations. Historically they all are used in climate or weather forecast models of Institute of Numerical Mathematics of the Russian Academy of Sciences [19, 57, 59] as well as in the other well-known models [37, 44]. As it is demonstrated bellow, the subgrid forces generate energy at all scales of backward energy cascade supporting large scale dynamics. This missing element must be restored in coarse models by some KEB parameterization. An *a priori* analysis of subgrid forces in this paper is analogues to the one in [43, 58]. We analyze three different KEB schemes. The first one is the stochastic KEB parameterization [8, 15, 52]. The second one is the linear deterministic 'negative eddy viscosity' scheme [15, 31] that was applied previously to similar models in [27, 28, 58]. In addition we test a subgrid model based on the scale-similarity [6, 38]. Note, that the scale-similarity subgrid model of [6] is very close to the nonlinear gradient model (see, e.g., [61]). The last one was already tested in *a priori* analysis of 2D turbulence [10, 41] where good correlation with subgrid forces was shown. Also in the former paper, stable modification of nonlinear gradient model is presented.

We evaluate the effects of subgrid parameterizations by comparing statistical characteristics of coarse models with the high resolution one. Statistics of interest are energy spectra and lagged auto correlation functions of the model solution. We also compare responses of the models to a steady state external forcing. Paper is structured as follows. In Section 2 we formulate model equations and introduce numerical discretization schemes. Section 3 is devoted to the *a priori* analysis of the DNS data. In Section 4 we describe KEB schemes and in Section 5 we present numerical results obtained with the coarse models. Summary of our results could be found in Section 6.

2 Model equations and parameters

Let us consider dynamics of the 2D incompressible fluid in the rectangular box $(x_1, x_2) \in [0, 2\pi) \times [0, 2\pi)$ on the non rotating plane with periodic boundary conditions. The amount of nodes (for coarse versions of the model) is 360 in both directions (discretization steps are (h_{x_1}, h_{x_2})). In the DNS simulation we use 2160×2160 resolution. With particular set of model variables (i.e., velocity-pressure or streamfunction-vorticity) the equations of motion are as follows:

$$\begin{cases} \dfrac{\partial \mathbf{u}}{\partial t} + (\mathbf{u} \cdot \nabla)\,\mathbf{u} = -\nabla p - \mu \Delta^2 \mathbf{u} - \alpha \mathbf{u} + \mathbf{f} \\ \nabla \cdot \mathbf{u} = 0, \end{cases} \qquad \begin{cases} \dfrac{\partial \omega}{\partial t} + J(\psi, \omega) = -\mu \Delta^2 \omega - \alpha \omega + f \\ \Delta \psi = \omega \end{cases} \tag{2.1}$$

Here $\mathbf{u} = (u, v)$, p, ψ, ω are the velocity, pressure, streamfunction, and vorticity, respectively. Laplacian, gradient, and Jacobian operators are Δ, ∇, and $J(\psi, \omega) = -\frac{\partial \psi}{\partial x_2}\frac{\partial \omega}{\partial x_1} + \frac{\partial \psi}{\partial x_1}\frac{\partial \omega}{\partial x_2}$, respectively, while $(\cdot)$ denotes inner product of 2D vectors. Bold symbols define the respective 2D vector fields. Variables in (2.1) are related to each other via the following expressions

$$\mathbf{u} = \left(-\frac{\partial \psi}{\partial x_2}, \frac{\partial \psi}{\partial x_1}\right), \qquad \omega = \frac{\partial v}{\partial x_1} - \frac{\partial u}{\partial x_2}. \tag{2.2}$$

2.1 Driving forcing and dissipative terms

External velocity forcing driving the turbulence in the model was taken in the form $\mathbf{f} = [a, b]^T \sin(\mathbf{k} \cdot \mathbf{x} + \varphi)$ (vorticity forcing f could be found using relations (2.2)) with the norm of the wave vector $\mathbf{k} = (k_1, k_2)$ being

close to $|\mathbf{k}| \approx k_f = 90$. The wave vector components (k_1, k_2) and the phase $\varphi \in [0, 2\pi]$ are chosen as discrete-time white noises. The power input per unit area averaged over one time step Δt could be evaluated according to [3]:

$$\varepsilon = \frac{\Delta t}{2}\left\langle f_{x_1}^2 + f_{x_2}^2 \right\rangle = \frac{\Delta t}{4}\left(a^2 + b^2\right) \tag{2.3}$$

where angle brackets stand for the time averaging. We fix energy source per unit area and unit time at the level of $\varepsilon = 1.5 \cdot 10^{-4}$, and for any (k_1, k_2, φ) we calculate a and b from (2.3) taking into account zero divergence condition for the forcing (i.e., $\nabla \cdot \mathbf{f} = 0$) giving additional linear relation for a and b.

Following ideas of [55] the background turbulence closure in (2.1) is represented by bi-harmonic damping. This is the common practice for the modelling of the large scale circulation of atmosphere and ocean where the dissipative terms are used to suppress numerical noise at short wave numbers. The coefficient μ was calculated according to the ideas of [34] as the enstrophy dissipation at small scales ($k > k_f$) must be equal to its generation by the random forcing provided that the KLB scaling theory (1.1) for the enstrophy is valid. This gives the functional formula for μ:

$$\mu = C_h \cdot \eta^{1/3} h^4 \tag{2.4}$$

where h is a grid step and $\eta = k_f^2 \varepsilon$ is the enstrophy source from the external forcing. Assuming that $C_b = 1.5$ in (1.1) (see high-resolved DNS results by [12]) and taking into account the finite difference approximation of biharmonic operator (see [45] for complete numerics), we obtain $C_h = 8.54 \cdot 10^{-2}$ and the corresponding values of coefficients μ which provide identical enstrophy dissipations for an ideal power law spectra in direct cascades: $\mu = 2.26 \cdot 10^{-9}$ (for the coarse model setup with resolution 360×360) and $\mu = 1.64 \cdot 10^{-12}$ (for DNS model with resolution 2160×2160). The Rayleigh friction coefficient is $\alpha = 0.012$ for both high and low resolution models and was chosen this way to ensure that the backward energy cascade is long enough in spectral domain.

2.2 Numerical schemes

Spatial approximation for the model written in terms of velocity-pressure variables was accomplished in the following way. We use projection method [13] to approximate (2.1). Firstly, we find intermediate value of the velocity ($\mathbf{u}'$) approximating half step variables with the second order Adams–Bashforth method (for any φ: $\varphi^{n+1/2} = \frac{3}{2}\varphi^n - \frac{1}{2}\varphi^{n-1}$):

$$\frac{\mathbf{u}' - \mathbf{u}^n}{\Delta t} = -\left[(\mathbf{u} \cdot \nabla)\,\mathbf{u}\right]_h^{n+1/2} - \nabla_h p^n - \mu \Delta_h^2 \mathbf{u}^{n+1/2} - \alpha \mathbf{u}^{n+1/2} + \mathbf{f}^n. \tag{2.5}$$

Secondly, we project solution onto non divergent vector field space and renew the pressure. The low values of the Courant number is used (CFL $= \Delta t U_{\max}/h < 0.2$) to make our results independent of particular choice of a time integration method. Let us introduce finite difference operators:

$$\delta_{x_i}(\varphi) = \frac{\varphi(x_i + h_{x_i}/2) - \varphi(x_i - h_{x_i}/2)}{h_{x_i}}, \qquad \overline{\varphi}^{x_i} = \frac{\varphi\left(x_i + h_{x_i}/2\right) + \varphi(x_i - h_{x_i}/2)}{2}, \quad i = 1, 2. \tag{2.6}$$

Several methods for spatial approximation are tested.

– *Scheme* E. The scheme used in the INMOM ocean model [19] is constructed for Arakawa C-grid

$$\left[(\mathbf{u} \cdot \nabla) u_i\right]_h = \delta_{x_j}\left(\overline{u_j}^{x_i}\overline{u_i}^{x_j}\right) \tag{2.7}$$

where summation over repeated indices is assumed. Provided existence of numerical analogue for the continuity equation, the scheme E has analogue of energy conservation law [39].

– *Scheme* INMCM. Being one of the Arakawa-type schemes [5] the INMCM is used in the atmospheric component of the climate model INMCM5 [59]. The scheme is written as a linear combination of advection approximated in the two coordinate systems

$$\left[(\mathbf{u} \cdot \nabla) u_i\right]_h = \frac{2}{3}\overline{\overline{u_j}^{x_i}\delta_{x_j} u_i}^{x_j} + \frac{1}{3}\overline{u_j' \delta_{x_j'} u_i}^{x_j'} \tag{2.8}$$

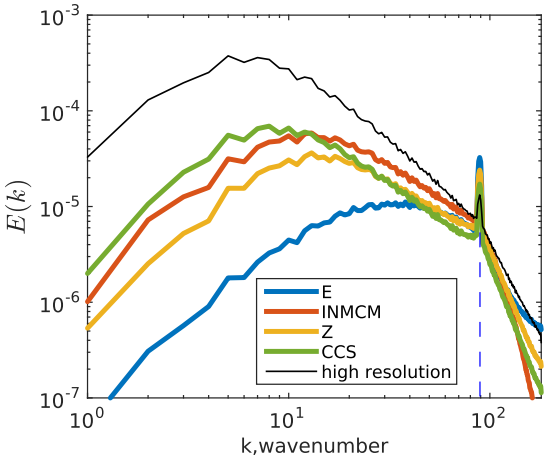

Fig. 1: The power spectrum of the DNS (black) and coarse models (blue – scheme E, red – scheme INMCM, yellow – Z, green – CCS).

where (u_1', u_2') is the velocity in the coordinate system (x_1', x_2') rotated by 45 degrees with respect to the original coordinate system (x_1, x_2).

For the numerical integration of (2.1) written in terms of streamfunction–vorticity variables we again use Adams–Bashforth scheme to approximate evolution equation for the vorticity. Next we update streamfunction by solving Poisson equation. The following spatial approximation methods were implemented.

- *Scheme* Z. Another Arakawa [4] scheme with second order central difference approximation for the advective nonlinear term $J(\psi, \omega)$ with skew-symmetric property conserving numerical analogue of the enstrophy.
- *Scheme* CCS. Cascade finite volume semi-lagrangian scheme CCS [42] is used in the prognostic atmospheric model SL-AV [57]. The CCS has the property of the total vorticity conservation. In our study the CCS is used with CFL = 0.6.
- The DNS model is written in terms of Z scheme.

2.3 Reproduction of the DNS spectra with coarse models

The DNS and coarse models were integrated from zero initial conditions for $T = [0, 200]$ (it is enough for the model to reach statistical equilibrium). Then we run the models for additional $T = [200, 1200]$ and store their solution for further analysis. The DNS solution power spectrum is shown in Figure 1 (black line). Here the forcing scale ($k_f = 90$) is marked by the dashed vertical line and only the scales with $k < 180$ are shown. Corresponding power spectra of coarse models are shown by colored lines (blue – scheme E, red – INMCM, yellow – Z, green – CCS). The evident conclusion from Fig. 1 is that in the equilibrium state all coarse models have much less energy in the large and intermediate scales (from 32% of the DNS level in the case of INMCM to 14% for E). We suppose that the source of this problem is suppression of the inverse energy cascade due to the damped medium scales and damped/unresolved small scales. Next two sections are devoted to the construction of parameterizations able to reduce this error.

3 Analysis of subgrid forces in the DNS model

3.1 Subgrid forces

Let $\overline{\omega}$ be a coarse grid vorticity obtained from the high resolution one (ω) by applying spatial filtration (i.e., the $\overline{(\cdot)}$ operator) that zeroes Fourier coefficients of the vorticity field outside the $[-k_{\max}, k_{\max}] \times [-k_{\max}, k_{\max}]$ spectral area. The discrete Fourier transformation maps $\overline{\omega}$ uniquely to the $N \times N$ grid of the coarse model ($N =$

$2k_{\max}$). We assume that we can act on $\overline{\omega}$ by either differential or coarse grid finite-difference operators (see [26] for details).

For the analysis of subgrid forces we consider the advection terms only. Let us first obtain dynamic equation for the $\overline{\omega}$ by filtering (2.1):

$$\begin{aligned} \frac{\partial \overline{\omega}}{\partial t} &= -\overline{J(\psi,\omega)} + \dots = -\left[J\left(\overline{\psi},\overline{\omega}\right)\right]_h + \sigma^{\omega} + \dots \\ \sigma^{\omega} &= \left[J\left(\overline{\psi},\overline{\omega}\right)\right]_h - \overline{J(\psi,\omega)}. \end{aligned} \tag{3.1}$$

Here we separated $\overline{J(\psi,\omega)}$ into two parts: $\left[J\left(\overline{\psi},\overline{\omega}\right)\right]_h$ stands for applying spatial approximation to coarse grid, the rest (σ^{ω}) is referred as the 'subgrid forces'. In the case of velocity-pressure variables we have similar formulas

$$\begin{aligned} \frac{\partial \overline{\mathbf{u}}}{\partial t} &= -\overline{(\mathbf{u}\cdot\nabla)\,\mathbf{u}} + \dots = -\left[(\overline{\mathbf{u}}\cdot\nabla)\,\overline{\mathbf{u}}\right]_h + \boldsymbol{\sigma}^{u} + \dots \\ \boldsymbol{\sigma}^{u} &= \left[(\overline{\mathbf{u}}\cdot\nabla)\,\overline{\mathbf{u}}\right]_h - \overline{(\mathbf{u}\cdot\nabla)\,\mathbf{u}}. \end{aligned} \tag{3.2}$$

The subgrid forces could be further separated into two parts, i.e., the effects of unresolved scales (the first term in the equation below) and approximation errors (the second term):

$$\boldsymbol{\sigma}^{u} = \{(\overline{\mathbf{u}}\cdot\nabla)\,\overline{\mathbf{u}} - \overline{(\mathbf{u}\cdot\nabla)\,\mathbf{u}}\} + \{\left[(\overline{\mathbf{u}}\cdot\nabla)\,\overline{\mathbf{u}}\right]_h - (\overline{\mathbf{u}}\cdot\nabla)\,\overline{\mathbf{u}}\}. \tag{3.3}$$

Approximation errors are zero for spectral methods but could play an important role in the case of finite-difference approximation methods [26].

3.2 Spectral properties of subgrid forces

Using the data from the DNS run described in Section 2.3 and applying decomposition (3.1), (3.2) we calculated statistical characteristics of resolved advection (calculated using coarse-grained fields and particular numerical scheme, i.e., $[(\overline{\mathbf{u}}\cdot\nabla)\overline{\mathbf{u}})]_h$) and subgrid forces. To be consistent with the resolution of the coarse models introduced above we use the same 360×360 resolution for the coarse-grained tendencies and variables. Three finite difference schemes (E, INMCM, and Z) were used to calculate time averaged power spectrum of resolved advection tendency (Fig. 2a) and the spectrum of the energy generation (Fig. 2b) by subgrid forces (i.e., $-2\pi k\mathrm{Re}\,\langle\psi_k^*\sigma_k\rangle$). The results for CCS scheme are not presented here as for the semi-lagrangian approximation we cannot extract coarse and subgrid part of the advection by applying simple spatial averaging formula (3.2).

From Fig. 2a we see that for the all three schemes the full DNS advection tendency ($J(\psi,\omega)$) could be well reproduced by its coarse-grained part ($[J(\overline{\psi},\overline{\omega})]_h$) in large scales. However at the small scales subgrid part of advection is important (note the difference at the right end of the spectrum between black and colored curves in Fig. 2a). Apart from the frequency cutoff effect, the numerical scheme approximation errors could also contribute here. Analogous results were also obtained in [32].

Despite the advection at large scales is correctly approximated by the coarse-grained part of the tendency, the equilibrium dynamics of coarse models could be very different from the DNS one. The reason is missing energy generation produced by the subgrid forces (see Fig. 2b). In the equilibrium state they generate as much as 55% of the total energy supplied by the external forcing to backward cascade scales ($k < 90$). At the same time for direct enstrophy cascade scales ($k > 90$) subgrid forces provide enstrophy dissipation. This energy generation is nothing else that KEB from subgrid forces and it has similar shape for all three numerical schemes considered. The maxima of the energy generation curve is located in the middle of the inverse energy cascade interval. Therefore, subgrid forces systematically inject energy in a wide range of scales. If missed in coarse models, it leads to the degradation of large scale circulation on 'climate' time scales due to the Rayleigh friction as shown in Fig. 1.

Most of the missing energy generations in Fig. 2b correspond to the scheme numerical errors (i.e., the second term of the right hand side of (3.3)) contributing to about 2/3 out of the 55% of the total energy generation deficit while the rest is due to the missing interactions with subgrid scales. The net subgrid forces

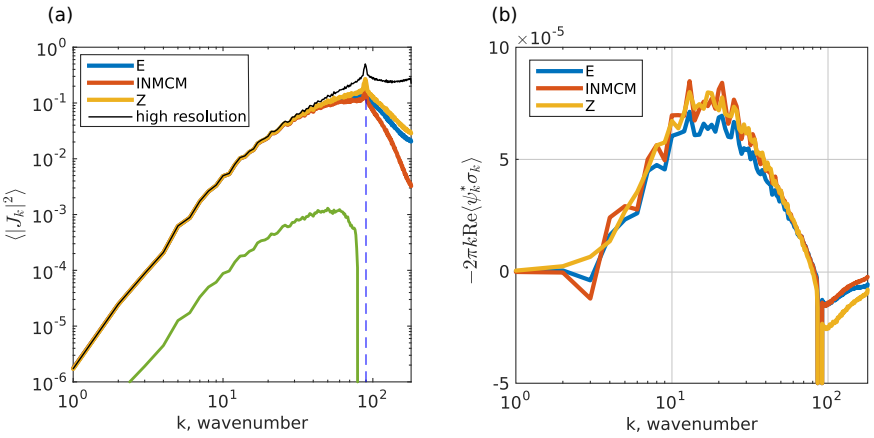

Fig. 2: The spectrum (a) of the advection for the DNS solution (log-log scales). Black line indicates full DNS tendency, colored lines show advection spectrum of large (coarsened) scales obtained using three different numerical schemes (blue – scheme E, red – scheme INMCM, yellow – scheme Z). Energy generation (b) of subgrid forces (log-linear scales) for the DNS model (blue – scheme E, red – scheme INMCM, yellow – scheme Z). Green line corresponds to stochastic parameterization and shown to indicate its small magnitude.

energy generation quickly decreases with the increase of the resolution of the coarse-grained solution. Analogous calculations for the 720×720 resolution give the value of subgrid forces energy generation of just 15% (instead of 55%) from the total.

3.3 Scale self similarity assumption

Let us assume that subgrid forces (3.2) can be represented in a divergent form:

$$\sigma_i^u = -\delta_{x_j}\left(\tau_{ij}^u\right)$$

where τ_{ij}^u is the tensor taking into account both stresses induced by resolved-subgrid interactions and stresses related to the approximation errors. To approximate τ_{ij}^u we borrow one of the most popular nonlinear subgrid closures in 3D LES modelling. Namely, we use the so called scale-similarity approach proposed and tested in [6]:

$$\tau_{ij}^{u,L} = \overline{u_i u_j}^L - \overline{u_i}^L \overline{u_j}^L \approx \overline{\overline{u_i}^L \overline{u_j}^L}^L - \overline{\overline{u_i}^L}^L \overline{\overline{u_j}^L}^L \tag{3.4}$$

where $\overline{(\cdot)}^L$ is the LES model filter appearing in the standard LES model formulation. It is known that assumption (3.4) works well in the *a priori* 3D tests giving high correlation between modelled and real stresses [6]. It is also well known that (3.4) is dissipative overall but still can provide local energy generation. Similar family of closures could be obtained by using wider filter for the 'external' averaging (rather than the basic LES filter) together with the proper rescaling of the closure ($l_{ij}^{u,L}$ is the so-called Leonard tensor, see [24] for details):

$$\tau_{ij}^{u,L} \cong C_{\mathrm{sim}} l_{ij}^{u,L}, \qquad l_{ij}^{u,L} = \widetilde{\overline{u_j}^L \overline{u_i}^L} - \widetilde{\overline{u_j}^L}\,\widetilde{\overline{u_i}^L}. \tag{3.5}$$

Here $\widetilde{(\cdot)}$ is an additional ('external' or 'test') filter. Coefficient C_{sim} could be either obtained from dynamical consideration or calculated empirically [40, 60]. More detailed information on the use of Leonard tensor approach (3.5) in 3D LES modelling could be found in [38].

Adopting above ideas we suppose that scale-similarity approach can be used for modelling KEB in the 2D case as well. Note that in the 2D case this type of closures was not tested extensively. In the *a priori* tests we choose the LES model filter $\overline{(\cdot)}^L$ to be spectral one $\overline{(\cdot)}$. The test filter $\widetilde{(\cdot)}$ is based on three-point one-dimensional filtration:

$$F_{x_i}(\varphi) = a\,\varphi(x_i - h_{x_i}) + (1 - 2a)\varphi(x_i) + a\,\varphi(x_i + h_{x_i}) \tag{3.6}$$

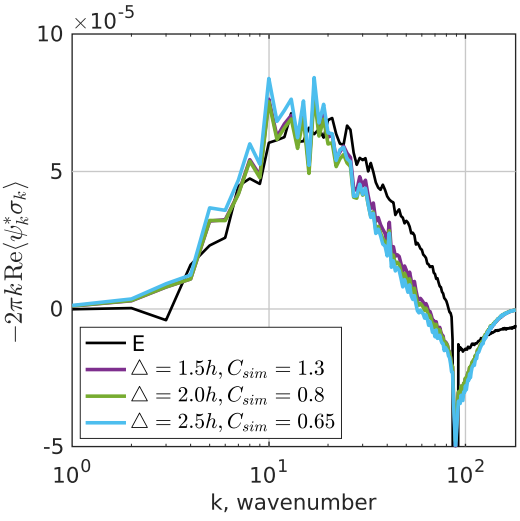

Fig. 3: The spectrum of the energy generation by subgrid forces in the model (black) as well as the Leonard tensors obtained for 2.5 grid step filter (light blue), 2 grid step filter (green), and 1.5 grid step filter (purple). Corresponding optimal normalizations for the Leonard tensor are 0.65, 0.8, and 1.3 respectively.

where coefficient $a < 1/2$ defines the filter band width $\Delta_f/h_{x_i} = \sqrt{24a}$ according to [35]. As a result, for 2D test filter $\widetilde{(\cdot)}$ we have:

$$\widetilde{\varphi} \equiv F_{x_2}\left(F_{x_1}(\varphi)\right) = F_{x_1}\left(F_{x_2}(\varphi)\right). \tag{3.7}$$

The following parameterization of unresolved flux in (3.2) is considered:

$$\sigma_i^u = -C_{\mathrm{sim}}\delta_{x_j}\left(l_{ij}^u\right), \qquad l_{ij}^u = \widetilde{\widetilde{u_j}\,\widetilde{u_i}} - \widetilde{\widetilde{u_j}}\,\widetilde{\widetilde{u_i}} \tag{3.8}$$

where δ_{x_j} is defined on the grid of coarse model.

Let us illustrate this idea by calculating energy generation for model (3.8). Three test filters $\widetilde{(\cdot)}$ were used having the band widths of 1.5, 2, and 2.5 grid steps of coarse model h. In Fig. 3 we show the energy generation spectrum for these three cases ($\Delta_f = 1.5h$ – purple, $2.0h$ – green, $2.5h$ – light blue) together with the energy generation of E scheme subgrid forces (same as blue curve in Fig. 2b). Note that Leonard tensor energy generation in Fig. 3 was scaled by the C_{sim} equals to 1.3, 0.8, and 0.65 for $\Delta_f = 1.5h$, $2.0h$, and $2.5h$, respectively. From Fig. 3 we may conclude that Leonard tensor gives the correct functional dependence for the subgrid forces and can be used as a KEB parameterization provided its amplitude C_{sim} is adjusted and it is used for sufficiently large scales.

4 Kinetic energy backscatter parameterizations

From our results shown in Section 2.3 it is evident that the coarse models are unable to represent the model dynamics correctly having insufficient inverse energy cascade and damped large scale circulation modes. Below we will consider several methods based on the analysis of the DNS model solution to fix this problem.

4.1 Purely stochastic parameterization

Stochastic energy backscatter parameterization considered in this section is based on the auto regression model in the Fourier space as in paper [8]. Model parameters are calculated from the energy generation spectrum of the DNS experiment.

Let us write equation (2.1) in Fourier space assuming some time approximation

$$\frac{\omega_k^{n+1} - \omega_k^n}{\Delta t} = F_k^n + s_k^n \tag{4.1}$$

where F_k^n is responsible for all dynamical processes, s_k^n is a stochastic parameterization, n is the time step number and k is the Fourier wavenumber. The stochastic tendency s_k^n will be modelled by the AR1 process [56]

as

$$s_k^{n+1} = \beta_k s_k^n + d_k \varepsilon_k^n$$

with damping coefficient $\beta_k \in [0, 1)$, ε_k^n is a white noise with unit variance and d_k is its amplitude multiplier. From the analysis of subgrid forces it follows that the correlations between its Fourier components are negligible, so we choose ε_k^n to be statistically independent for different k. For the noise and the AR1 covariance matrices we have [56]:

$$\left\langle \varepsilon_k^m \varepsilon_k^{n*} \right\rangle = \delta_{m,n}, \qquad \left\langle s_k^m s_k^{n*} \right\rangle = \beta_k{}^{|m-n|} \frac{d_k^2}{1-\beta_k^2}. \tag{4.2}$$

In the above equations the asterisk denotes complex conjugation while angle brackets stand for the averaging over the process realizations. From (4.2) we can obtain correlation time τ_d^k and variance of the process s_k^n in the form

$$\tau_k^d = \frac{\Delta t}{1-\beta_k}, \qquad \left\langle s_k^n s_k^{n*} \right\rangle = \frac{d_k^2}{1-\beta_k^2}. \tag{4.3}$$

Let us estimate the contribution of stochastic forcing s_k^n to the energy budget. According to [3, 54], energy ($E_k = \omega_k \omega_k^* / (2k^2)$) production rate during small temporal interval Δt provided by stochastic term is the following

$$k^2 \frac{\Delta E_k}{\Delta t} = \mathrm{Re}\left(\omega_k^n s_k^{n*}\right) + \frac{\Delta t}{2} s_k^n s_k^{n*}. \tag{4.4}$$

Right hand side of the above equation could be expressed in terms of s_k^n only using (4.1) as $\omega_k^n = \Delta t \sum_{m=0}^{n-1} (s_k^m + F_k^m)$. After substitution of the last expression into (4.4), assuming that $\left\langle s_k^n F_k^{m*} \right\rangle = 0$ (see also, [8]) and performing summation over m index with the use of (4.2) we have:

$$k^2 \left\langle \frac{\Delta E_k}{\Delta t} \right\rangle = \lim_{n\to\infty} \Delta t \left[\frac{1}{2} \left\langle s_k^n s_k^{n*} \right\rangle + \sum_{m=0}^{n-1} \left\langle s_k^m s_k^{n*} \right\rangle \right] = \frac{\Delta t}{2} \frac{d_k^2}{(1-\beta_k)^2}. \tag{4.5}$$

Stochastic parameterization damping value β_k is chosen to make τ_d^k close to the e^{-1} decay time of subgrid forces lagged autocorrelation function which is wavenumber-dependent and decreases as the wavenumber increases. In turns, noise amplitude d_k is obtained from the equation $-\mathrm{Re}\left\langle \psi_k \sigma_k^* \right\rangle = \langle \Delta E_k / \Delta t \rangle$ for energy inflow from the subgrid forces assuming that all this inflow is provided by stochastic parameterization given by (4.5).

Note that inequality

$$k^2 \left\langle \frac{\Delta E_k}{\Delta t} \right\rangle = \tau_k^d (1+\beta_k) \frac{\left\langle s_k^n s_k^{n*} \right\rangle}{2} \geqslant \frac{1}{2} \tau_k^d \left\langle s_k^n s_k^{n*} \right\rangle$$

suggests that the noise variance is inversely proportional to the decorrelation time (provided energy flux is kept fixed). As a result, stochastic parameterization term has sufficiently small amplitude compared with the advection on large scales where the characteristic decorrelation time is of order of one hundred time steps (see the green curve in Fig. 2a).

Assuming that $s^\omega(\mathbf{x}, t)$ is the stochastic parameterization tendency constructed in the physical space, its $(\mathbf{u}, p)$-representation analogue will have the following form

$$(s_1^u, s_2^u) = \left(-\frac{\partial}{\partial x_2}, \frac{\partial}{\partial x_1} \right) \Delta^{-1} s^\omega(\mathbf{x}, t).$$

4.2 Negative viscosity approach

Let us follow [15, 31] and write down spectral linear viscosity model in the Fourier space

$$\frac{\partial \omega_k}{\partial t} = \cdots - \nu(k) k^2 \omega_k \tag{4.6}$$

where $\nu(k)$ is the eddy viscosity parameter. The net energy balance from this linear term can be written as

$$\left\langle \frac{\partial E_k}{\partial t} \right\rangle = \cdots - \nu(k) \left\langle \omega_k^* \omega_k \right\rangle.$$

With negative value of eddy viscosity parameter ($\nu(k) < 0$) we can describe missing energy generation in the model. For the sake of direct comparability between this approach and the stochastic one we define the eddy viscosity as

$$\nu(k) = -\left\langle \frac{\Delta E_k}{\Delta t} \right\rangle \Big/ \left\langle \omega_k^* \omega_k \right\rangle$$

where the energy generation spectra ($\langle \Delta E_k / \Delta t \rangle$) is taken from the stochastically driven models and the solution power spectra ($\langle \omega_k^* \omega_k \rangle$) is obtained from the coarse model.

4.3 Scale-similarity parameterization for the coarse model

For the numerical experiments with coarse models we have used scale-similarity parameterization which is slightly different from equation (3.8). For the $(\mathbf{u}, p)$ representation we have:

$$\sigma_i^u = -C_{\text{sim}} \delta_{x_j} \widehat{l_{ij}^u}, \qquad l_{ij}^u = \widetilde{u_j^h u_i^h} - \widetilde{u_j^h} \widetilde{u_i^h} \tag{4.7}$$

where u_j^h is the velocity in coarse model. The width Δ_f / h of test filter $\widetilde{(\cdot)}$ was chosen equal to 2 ($a = 1/6$ in equation (3.6)). Here we introduced additional spectral filtration $\widehat{(\cdot)}$ of the tensor l_{ij}^u that removes all scales smaller than $0.9 k_f$ ($k > 0.9 k_f$). This filtration is required to avoid spurious dissipation at small scales (see Fig. 3, large wave numbers). Analogous parameterization in terms of streamfunction–vorticity variables is:

$$\sigma^\omega = -C_{\text{sim}} \delta_{x_j} \widehat{l_j^\omega}, \qquad l_j^\omega = \widetilde{u_j^h \omega^h} - \widetilde{u_j^h} \widetilde{\omega^h}. \tag{4.8}$$

The C_{sim} constant must be different from the one calculated in Subsection 3.3 as it was obtained for the DNS data and cannot be used for the coarse models having sufficiently different small scale dynamics. Following values of C_{sim} for different schemes were chosen to equalize total energy generation of model (4.7), (4.8) to that of models (4.1) and (4.6): 4.1, 1.5, 2.3, 2.6 for schemes E, INMCM, Z, and CCS, respectively.

4.4 Combined stochastic and scale-similarity parameterization

The last parameterization tested here is the combined model, which is a linear combination of scale-similarity approach (4.7), (4.8) and stochastic one (4.1):

$$\sigma_i^u = C_{\text{stoch}} s_i^u - C_{\text{sim}} \delta_{x_j} \widehat{l_{ij}^u} \tag{4.9}$$

$$\sigma^\omega = C_{\text{stoch}} s^\omega - C_{\text{sim}} \delta_{x_j} \widehat{l_j^\omega}. \tag{4.10}$$

Specific approach for calculation of constants C_{stoch} and C_{sim} will be described below.

5 Numerical experiments and results

In this section we present numerical results on modelling 2D isotropic turbulence model based on the system (2.1). We integrate (2.1) using 4 different advection schemes (i.e., E, INMCM, Z, and CCS) starting from zero initial conditions until the statistical characteristics of model solution reach an equilibrium (the characteristic time scale of intermittent behavior is around 200 time units). During the next 1000 time units we collect statistics of the model solution for further comparison. As it was mentioned before, the spatial resolution of these numerical experiments is 360×360 and the forcing driving the system has characteristic length corresponding to wave number 90 (four mesh steps of coarse model). Together with the bare coarse model run for each numerical scheme we repeat the integration supplementing the model with one of the four parameterizations – pure stochastic KEB parameterization (Subsection 4.1), negative eddy viscosity (Subsection 4.2),

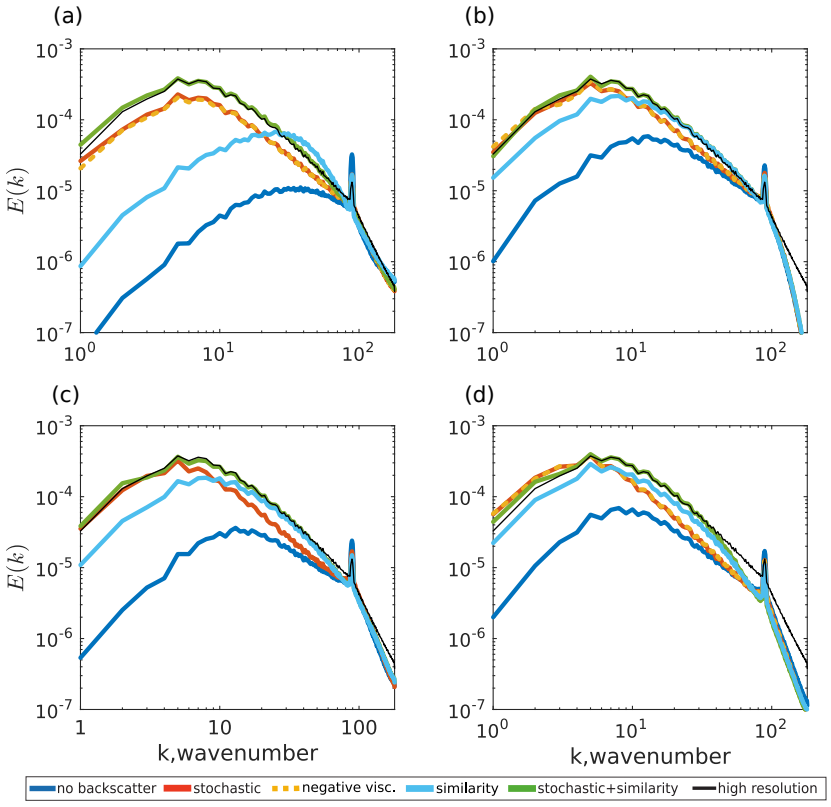

Fig. 4: The equilibrium power spectrum of the solution at coarse resolution obtained for 4 different numerical schemes ((a) – scheme E, (b) – scheme INMCM , (c) – scheme Z, (d) – scheme CCS): without parameterization (dark blue), stochastic parameterization only (red), negative viscosity parameterization (yellow), scale-similarity parameterization (light blue), stochastic parameterization and scale-similarity tendency (green). The equilibrium power spectrum of the DNS solution is shown by black curve.

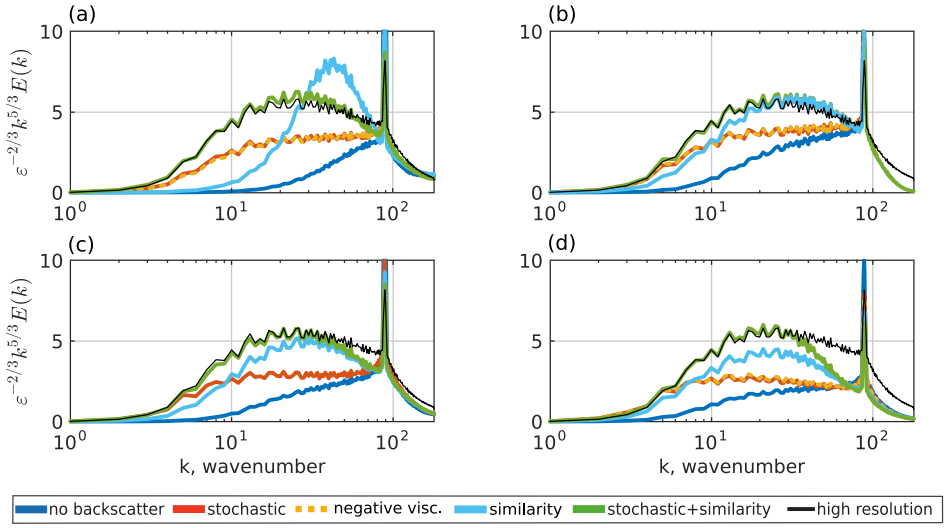

Fig. 5: The same as in Fig. 4, but energy spectrum is compensated (i.e., multiplied by the factor of $\varepsilon^{-2/3}k^{5/3}$).

similarity (Subsection 4.3) and combination of scale-similarity + stochastic approaches (Subsection 4.4). In all experiments with the stochastic KEB parameterization we use the same energy generation spectrum obtained for scheme Z in the *a priori* analysis, see Subsection 3.2 and Fig. 2b.

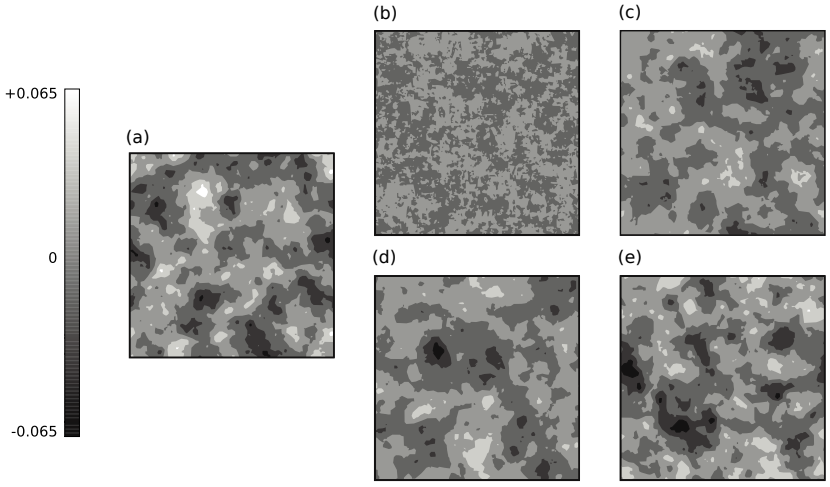

Fig. 6: The snapshot of the model solution (streamfunction) for DNS (a) and for the coarse model based on the scheme E without backscatter (b), with stochastic (c), negative viscosity (d) or combined parameterization (e).

In Figs. 4 and 5 one can see the energy spectra and their compensated counterparts (i.e., the ones scaled by the factor $\varepsilon^{-2/3}k^{5/3}$) of the coarse models in comparison with the reference DNS data represented by the same black curve in all plots. Subfigure (a) demonstrates the case of E scheme. Subfigures (b), (c), and (d) present the data for INMCM, Z, and CCS schemes, respectively. On each plot dark blue curve stands for the bare coarse model run while red one represents coarse model with stochastic parameterization (4.1), yellow curve shows the coarse model with negative viscosity parameterization (4.6), light blue line is the coarse model with scale-similarity parameterization (4.7), (4.8) and green line is the case where combined deterministic-stochastic approach (4.9), (4.10) is used.

According to the *a priori* analysis of subgrid forces they should transfer 55% of the forcing power to the scales larger than forcing scale. Actual transfer for stochastic parameterization in coarse models is slightly less (45%) due to inaccuracy of estimate (4.5). Due to this parameterization the energy of the largest scales with ($1 < k \leqslant 5$) becomes almost the same as the one in DNS (the total energy raised almost 4 times for the worst E scheme). In the middle scales ($5 < k < 90$) coarse models still have reduced energy values. Further increase of the stochastic forcing do not change the dynamics qualitatively – almost all additional energy goes to the largest scales making them unrealistically strong and leaving middle scales damped. Particularly, one needs to increase value of stochastic parameterization at least in four times to reach the required level of the middle scale energy in coarse models.

The effect of applying the negative viscosity parameterization looks almost identical but it has an additional disadvantage. Sometimes negative viscosity could be a source of exponential growth of the solution. For instance, we have documented this effect for the scheme Z when the amplitude of small vortices at the forcing scales grows uncontrollably. Spurious rise of small vortices due to negative viscosity approach was also mentioned in [27].

The scale-similarity parameterization (4.7), (4.8) cannot provide enough energy to large scales in most cases. However it effectively corrects power spectrum at middle scales (see light blue lines in Fig. 5). It is natural to suppose that the improved parameterization of KEB can be achieved using combined approach (4.9), (4.10). While the stochastic subgrid model corrects the large scale motions, the scale-similarity model restores the middle scales. The optimal values of the coefficients C_{stoch} and C_{sim} should be chosen individually for a given spatial resolution and numerical scheme of a coarse model. By varying these coefficients we have achieved the coincidence of the energy spectra for all four coarse models (green lines in Figs. 4 and 5) with DNS data (black lines) in the range ($1 < k < 40$). Values of C_{stoch} and C_{sim} are (1.25, 1.7), (0.79, 1.4), (0.76, 2.5), and (0.43, 4.0) for E, INMCM, Z, and CCS schemes, respectively. Under this choice of coefficients, the total energy generation produced by the combined parameterization appears to be nearly equal to the energy dissipation caused by biharmonic viscosity. Also the spectral density in the inertial energy range increases up

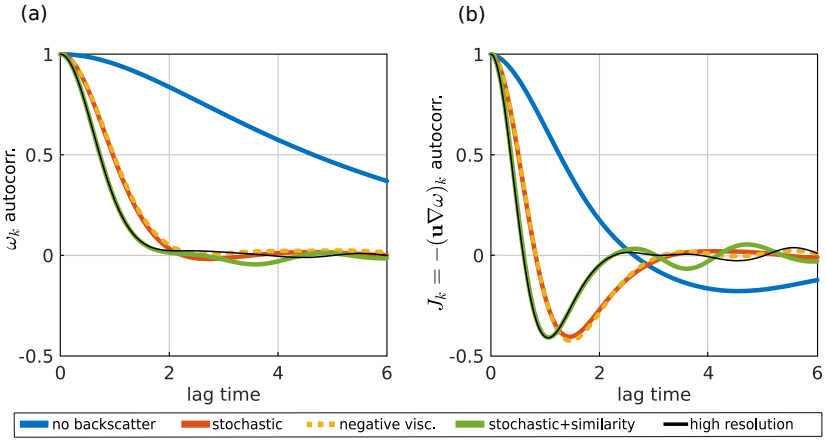

Fig. 7: Autocorrelation functions for Fourier components of vorticity (a) and advection (b) for wave number 30 obtained with the coarse model using scheme E: without parameterization (blue), stochastic parameterization only (red), negative viscosity parameterization (yellow), stochastic parameterization and scale-similarity tendency (green). Results for the DNS solution are shown by black curves.

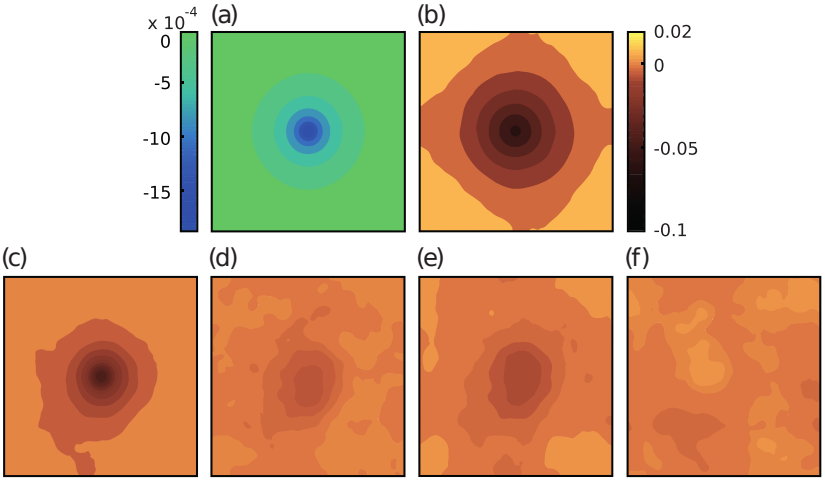

Fig. 8: Forcing perturbation (a) and correspondent time averaged response (stream function field) of the DNS model (b). Bottom row: coarse model (scheme E) response errors with respect to the DNS model response: bare coarse model (c), models with stochastic (d), negative viscosity (e) and combined (f) parameterization included.

to the level comparable with the one defined by the known evaluations of Kolmogorov constant $C_f \sim 6 \pm 0.5$ (see, e.g., [11]), which is much larger than the level provided by the stochastic or negative viscosity parameterizations ($C_f \sim 3 - 4$, red and yellow curves in Fig. 5). Two schemes (E and INMCM) correctly reproduce deviations of the spectra from the $-5/3$ power law almost everywhere in the range of wavenumbers left to the external forcing scale (see discussion in [9] for physical reasons of these deviations). Note that in the present paper we do not propose any formal algorithm for calculation of C_{stoch} and C_{sim} but simply show that the appropriate choice is possible.

It was checked (the results are not presented here) that the similar way of KEB parameterizations can be used to improve the spectra of coarse models with higher resolution (i.e., 540×540) where the level of initial errors is smaller (see [45]).

In Fig. 6a we show a typical snapshot of the DNS model streamfunction. Coarse model (based on scheme E) has almost zero large scale component (see Fig. 6b). Inclusion of stochastic term or negative viscosity improves the structure of the flow (see Fig. 6c and 6d). Combined approach (see Fig. 6e) gives the best results.

Tab. 1: Relative error of the averaged streamfunction response of the coarse models onto the perturbation. Level of significance is 0.04.

	$\|\|\langle\psi\rangle - \langle\psi_{DNS}\rangle\|\|_\infty / \|\|\langle\psi_{DNS}\rangle\|\|_\infty$				$\|\|\langle\psi\rangle - \langle\psi_{DNS}\rangle\|\|_2 / \|\|\langle\psi_{DNS}\rangle\|\|_2$			
Parameterization/Scheme	**E**	**INMCM**	**Z**	**CCS**	**E**	**INMCM**	**Z**	**CCS**
bare coarse model	0.83	0.47	0.68	0.58	0.44	0.30	0.39	0.37
stochastic	0.13	0.08	0.09	0.10	0.13	0.11	0.10	0.11
negative viscosity	0.17	0.09	unstable	0.11	0.19	0.13	unstable	0.14
stochastic+similarity	0.07	0.08	0.05	0.05	0.11	0.10	0.07	0.08

Another important statistical property of the model is the lagged auto covariance function characterizing rate of anomaly decorrelation in the system. In Fig. 7 we present the lagged auto correlation for the Fourier components ($k = 30$, middle scales) of vorticity ω_k (left frame) and advection term $J_k = -(\mathbf{u}\cdot\nabla\omega)_k$ (right frame). From Fig. 7 it follows again that stochastic parameterization improves characteristic variability times in the model and the shape of the lagged correlations. Reduction of these time scales could be due to the emergency of the large scale advection. With combined approach the middle scale dynamics gets another improvement.

For the climate modelling problems we would like to use models having the same sensitivity properties as the real climate system. At least it is crucially important for the climate change forecast when the system reaction on external forcings has to be predicted. Therefore, it would be very desirable for the coarse model to have the same sensitivity as the DNS which is very nontrivial requirement [2]. To compare response properties of the coarse models and DNS we apply a small (with respect to advective term) constant in time perturbation to the right hand side of (2.1):

$$\frac{\partial\omega}{\partial t} = \cdots + 0.09 \cdot \exp(-70 \cdot [(x_1 - \pi)^2 + (x_2 - \pi)^2]). \tag{5.1}$$

The response was calculated using averaging over 24000 time units. The perturbation (a), DNS response (b), and coarse model (scheme E) response errors (c)–(f) are shown in Fig. 8.

Coarse models without parameterization (see Fig. 8c) give the errors comparable with the reference DNS response (see norms of these errors presented in Table 1). The use of the stochastic parameterization improves response (see Fig. 8d) and reduces the norms of errors (Table 1). Model with negative viscosity parameterization (see Fig. 8e) gives worse results compared to the stochastic one. Combined parameterization (see Fig. 8f) gives almost perfect results both for the maximum ($\|\cdot\|_\infty$) and root mean square ($\|\cdot\|_2$) response values.

6 Conclusions

In the present paper we considered several approaches to the modelling of large scale dynamics produced by the forced isotropic two-dimensional turbulence. As a particular problem we analyze stationary bidirectional energy and enstrophy cascade in the viscous incompressible fluid with the energy dissipation at large scales provided by the Rayleigh friction.

When the spatial scale of generating energy source is close to the grid step (the mesh is supposed to have relatively coarse resolution) numerical models are unable to reproduce backward energy cascade and the amplitude of large scales correctly. The main reason of this error is due to the fact that essential part of the backward cascade at large and medium scales is supported by triad interactions involving unresolved scales or small scales misrepresented by the numerical schemes. Typical way to correct coarse grid numerical models is to use one or another subgrid parameterization for backward redistribution of kinetic energy (or kinetic energy backscatter, KEBs).

First, we verified the standard approaches to model KEBs, namely stochastic parameterization (SKEBs) and linear subgrid model using the negative viscosity approximation. These two parameterizations were tested for four numerical approximation schemes having different number of quadratic invariants. Param-

eters of the subgrid parameterizations took into account results of high resolution (DNS) simulation and specifics of the particular numerical scheme used in the model. We have shown that subgrid models indeed help to increase the energy of large scales and make it close to the one in DNS. In addition, the autocorrelation functions of model variables as well as response properties of coarse models to external perturbations were all improving. On the other hand, one common problem still exists – both subgrid models are unable to translate enough energy to middle scales preventing better correspondence of large and middle scales statistics with respect to DNS. Also, the negative viscosity model produces numerical instability for one of the approximation schemes.

Further improvements could be obtained when we complement SKEBs with the deterministic nonlinear subgrid parameterization aimed to improve dynamics at middle scales. This parameterization is based on the so-called scale-similarity hypothesis widely used in large eddy simulations of 3D turbulent flows. The *a priori* analysis of the DNS solution has shown that it produces energy generation in middle scales similar in shape to the one produced by the subgrid forces estimated for one or another approximation scheme. It was found that the scale-similarity model is overly dissipative at small scales and must be filtered out at this spectral region. As a result, with the proper choice of coefficients regulating amplitude of the stochastic and nonlinear deterministic parameterizations, one can obtain almost exact correspondence between the energy spectra of DNS and coarse resolution models. In addition, the characteristic times of large and middle scales were improved in all coarse models as can be seen from the shapes of the auto correlation functions. Coarse models equipped with the combined parameterization have almost the same sensitivity to external perturbations as the high resolution model that is very useful for climate modelling and climate change problems.

We should also mention several potential disadvantages of the suggested approach. First, we have to adjust the set of parameters for every particular numerical approximation scheme used in the model. Second, we used Fourier space (and Fourier transform) for constructing subgrid parameterizations making it difficult to directly apply our results to spatially non isotropic case (boundary currents, rotation etc.). Possible ways to remove (or reduce) these difficulties could be the use of the discrete filters with compact support and simplified stochastic parameterization. In turns, parameters of the combined closure could be estimated using dynamic procedure from [25].

Funding: This work was supported by the Russian foundation for Basic Research (projects 16-55-12015, 18-05-60126, 18-05-60184).

References

[1] U. Achatz and G. Branstator, A two-layer model with empirical linear corrections and reduced order for studies of internal climate variability. *J. Atmos. Sci.* **56** (1999), No. 17, 3140–3160.
[2] U. Achatz, U. Löbl, S. Dolaptchiev, and A. Gritsun, Fluctuation–dissipation supplemented by nonlinearity: a climate-dependent subgrid-scale parameterization in low-order climate models. *J. Atmos. Sci.* **70** (2013), No. 6, 1833–1846.
[3] K. Alvelius, Random forcing of three-dimensional homogeneous turbulence. *Phys. Fluids* **11** (1999), No. 7, 1880–1889.
[4] A. Arakawa, Computational design for long-term numerical integration of the equations of fluid motion: Two-dimensional incompressible flow. Part I. *J. Comput. Phys.* **1** (1966), No. 1, 119–143.
[5] A. Arakawa and V. Lamb, Computational design of the basic dynamical processes of the UCLA general circulation model. *Methods Comput.l Phys.* **17** (1977), 173–265.
[6] J. Bardina, J. Ferziger, and W. Reynolds, Improved subgrid-scale models for large-eddy simulation. In: *13th Fluid and Plasma Dynamics Conference*. 1980, p. 1357.
[7] G. Batchelor, Computation of the energy spectrum in homogeneous two-dimensional turbulence. *The Physics of Fluids* **12** (1969), No. 12, II-233–II-239.
[8] J. Berner, G. Shutts, M. Leutbecher, and T. Palmer, A spectral stochastic kinetic energy backscatter scheme and its impact on flow-dependent predictability in the ECMWF ensemble prediction system. *J. Atmos. Sci.* **66** (2009), No. 3, 603–626.
[9] B. Burgess, R. Scott, T. Shepherd, Kraichnan–Leith–Batchelor similarity theory and two-dimensional inverse cascades. *J. Fluid Mech.* **767** (2015), 467–496.
[10] F. Bouchet, Parameterization of two-dimensional turbulence using an anisotropic maximum entropy production principle (2003). arXiv:cond-mat/0305205

[11] G. Boffetta and S. Musacchio, Evidence for the double cascade scenario in two-dimensional turbulence. *Physical Review E*, **82** (2010), No. 1, 016307.
[12] G. Boffetta and R. Ecke, Two-dimensional turbulence. *Annual Review of Fluid Mech.*, **44** (2012), 427–451.
[13] D. Brown, R. Cortez, and M. Minion, Accurate projection methods for the incompressible Navier–Stokes equations. *J. Comp. Phys.* **168** (2001), No. 2, 464–499.
[14] P. Chavanis, A parametrization of two-dimensional turbulence based on a maximum entropy production principle with a local conservation of energy. *Fluid Dynamics Research* **46** (2014), No. 6, 061409.
[15] J. Chasnov, Simulation of the Kolmogorov inertial subrange using an improved subgrid model. *Physics of Fluids A: Fluid Dynamics* **3** (1991), No. 1, 188–200.
[16] S. Danilov and D. Gurarie, Quasi-two-dimensional turbulence. *Physics-Uspekhi*, **43** (2000), No. 9, 863–900.
[17] J. Deardorff, A numerical study of three-dimensional turbulent channel flow at large Reynolds numbers. *J. Fluid Mech.* **41** (1970), No. 2, 453–480.
[18] S. Dolaptchiev, U. Achatz, and I. Timofeyev, Stochastic closure for local averages in the finite difference discretization of the forced Burgers equation. *Theor. Comput. Fluid Dynamics* **27** (2013), No. 3-4, 297–317.
[19] N. Diansky, A. Bagno, and V. Zalesny, Sigma model of global ocean circulation and its sensitivity to variations in wind stress. *Izv. Atmos. Ocean. Phys.* **38** (2002), No. 4, 477–494.
[20] V. Dymnikov, Dynamics of the two-dimensional ideal incompressible fluid and Casimirs. *Izv. Atmos. Ocean. Phys.* **52** (2016), No. 4, 348–352.
[21] V. Dymnikov and P. Perezhogin, Systems of hydrodynamic type that approximate two-dimensional ideal fluid equations. *Izv. Atmos. Ocean. Phys.* **54**, No. 3, 232–241.
[22] C. Franzke and A. Majda, Low-order stochastic mode reduction for a prototype atmospheric GCM. *J. Atmos. Sci.* **63** (2006), No. 2, 457–479.
[23] J. Frederiksen and A. Davies, Eddy viscosity and stochastic backscatter parameterizations on the sphere for atmospheric circulation models. *J. Atmos. Sci.* **54** (1997), No. 20, 2475–2492.
[24] M. Germano, A proposal for a redefinition of the turbulent stresses in the filtered Navier–Stokes equations. *The Physics of Fluids* **29** (1986), No. 7, 2323–2324.
[25] M. Germano, U. Piomelli, P. Moin, and W. Cabot, A dynamic subgrid-scale eddy viscosity model. *Physics of Fluids A: Fluid Dynamics* **3** (1991), No. 7, 1760–1765.
[26] S. Ghosal, An analysis of numerical errors in large-eddy simulations of turbulence. *J. Comput. Phys.* **125** (1996), No. 1, 187–206.
[27] M. Jansen and I. Held, Parameterizing subgrid-scale eddy effects using energetically consistent backscatter. *Ocean Modelling* **80** (2014), 36–48.
[28] M. Jansen, I. Held, A. Adcroft, and R. Hallberg, Energy budget-based backscatter in an eddy permitting primitive equation model. *Ocean Modelling* **94** (2015), 15–26.
[29] R. Kraichnan, Inertial ranges in two-dimensional turbulence. *The Physics of Fluids* **10** (1967), No. 7, 1417–1423.
[30] R. Kraichnan, Inertial-range transfer in two-and three-dimensional turbulence. *J. Fluid Mech.* **47** (1971), No. 3, 525–535.
[31] R. Kraichnan, Eddy viscosity in two and three dimensions. *J. Atmos. Sci.* **33** (1976), No. 8, 1521–1536.
[32] J. Laval, B. Dubrulle, and S. Nazarenko, Nonlocality of interaction of scales in the dynamics of 2D incompressible fluids. *Physical Review Letters* **83** (1999), No. 20, 4061–4064.
[33] C. Leith, Diffusion approximation for two-dimensional turbulence. *The Physics of Fluids* **11** (1968), No. 3, 671–672.
[34] D. Lilly, The representation of small scale turbulence in numerical simulation experiments. In: *Proc. of IBM Scientific Computing Symp. Environ. Sci.* 1967, pp. 195–210.
[35] T. Lund, On the use of discrete filters for large eddy simulation. In: *Annual Research Briefs. Center for Turbulence Research, NASA Ames-Stanford University.* 1997, pp. 83–95.
[36] A. Majda, I. Timofeyev, and E. Vanden Eijnden, A mathematical framework for stochastic climate models. *Comm. Pure App. Math.* **54** (2001), No. 8, 891–974.
[37] G. Mellor, *Users guide for a three dimensional, primitive equation, numerical ocean model*. Program in Atmospheric and Oceanic Sciences. Princeton University, Princeton, 1998.
[38] C. Meneveau and J. Katz, Scale-invariance and turbulence models for large-eddy simulation. *Annual Review of Fluid Mechanics* **32** (2000), No. 1, 1–32.
[39] Y. Morinishi, T. Lund, O. Vasilyev, and P. Moin, Fully conservative higher order finite difference schemes for incompressible flow. *J. Comp. Phys.* **143** (1998), No. 1, 90–124.
[40] Y. Morinishi and O. Vasilyev, A recommended modification to the dynamic two parameter mixed subgrid scale model for large eddy simulation of wall bounded turbulent flow. *Phys. Fluids.* **13** (2001), No. 11, 3400—3410.
[41] B. Nadiga, Orientation of eddy fluxes in geostrophic turbulence. *Philosophical Transactions of the Royal Society of London A: Mathematical, Physical and Engineering Sciences.* **366** (2008), No. 1875, 2489–2508.
[42] R. Nair, J. Scroggs, and F. Semazzi, Efficient conservative global transport schemes for climate and atmospheric chemistry models. *Monthly Weather Review* **130** (2002), No. 8, 2059–2073.
[43] A. Natale and C. Cotter, Scale-selective dissipation in energy-conserving finite element schemes for two-dimensional turbulence. *Q. J. R. Meteorol. Soc.* **143** (2017), No. 705, 1734–1745.

[44] R. Pacanowski, K. Dixon, and A. Rosati, *The GFDL modular ocean model users guide. GFDL Ocean Group Tech. Report No. 2*, 1991.
[45] P. Perezhogin, A. Glazunov, E. Mortikov, and V. Dymnikov, Comparison of numerical advection schemes in two-dimensional turbulence simulation. *Russ. J. Numer. Anal. Math. Modelling.* **32** (2017), No. 1, 47–60.
[46] P. Perezhogin and V. Dymnikov, Equilibrium states of finite-dimensional approximations of a two-dimensional incompressible inviscid fluid. *Nonlinear Dynamics* **13** (2017), No. 1, 55–79. (In Russian)
[47] P. Perezhogin and V. Dymnikov, Modelling of quasi-equilibrium states of a two-dimensional ideal fluid. *Doklady Physics* **62** (2017), No. 5, 248–252.
[48] R. Robert and J. Sommeria, Statistical equilibrium states for two-dimensional flows. *J. Fluid Mech.* **229** (1991), 291–310.
[49] R. Sadourny and C. Basdevant, Parameterization of subgrid scale barotropic and baroclinic eddies in quasi-geostrophic models: Anticipated potential vorticity method. *J. Atmos. Sci.* **42** (1985), No. 13, 1353–1363.
[50] P. Sagaut, *Large Eddy Simulation for Incompressible Flows: An Introduction*. Springer, Heidelberg, 2005.
[51] R. Salmon, *Lectures on Geophysical Fluid Dynamics*. Oxford University Press, Oxford, 1998.
[52] G. Shutts, A kinetic energy backscatter algorithm for use in ensemble prediction systems. *Q. J. R. Meteorol. Soc.* **131** (2005), No. 612, 3079–3102.
[53] G. Shutts and T. Palmer, Convective forcing fluctuations in a cloud-resolving model: Relevance to the stochastic parameterization problem. *J. Climate* **20** (2007), No. 2, 187–202.
[54] G. Shutts, A stochastic convective backscatter scheme for use in ensemble prediction systems. *Q. J. R. Meteorol. Soc.* **141** (2015), No. 692, 2602–2616.
[55] J. Smagorinsky, General circulation experiments with the primitive equations: I. The basic equations. *Monthly Weather Review* **91** (1963), No. 3, 99–164.
[56] H. Storch and F. Zwiers, *Statistical Analysis in Climate Research*. Cambridge University Press, Cambridge, 2001.
[57] M. Tolstykh, V. Shashkin, and R. Fadeev, G. Goyman, Vorticity-divergence semi-Lagrangian global atmospheric model SL-AV20: dynamical core. *Geosci. Model Dev.* **10** (2017), No. 5, 1961–1983.
[58] J. Thuburn, J. Kent, and N. Wood, Cascades, backscatter and conservation in numerical models of two-dimensional turbulence. *Q. J. R. Meteorol. Soc.* **140** (2014), No. 679, 626–638.
[59] E. Volodin, E. Mortikov, S. Kostrykin, V. Galin, V. Lykossov, A. Gritsun, N. Diansky, A. Gusev, and N. Iakovlev, Simulation of the present-day climate with the climate model INMCM5. *Climate Dynamics* **49** (2017), No. 11-12, 3715–3734.
[60] B. Vreman, B. Geurts, and H. Kuerten, On the formulation of the dynamic mixed subgridscale model. *Phys. Fluids* **6** (1994), No. 12, 4057–4059.
[61] G. Winckelmans and H. Jeanmart, Assessment of some models for LES without/with explicit filtering. In: *Direct and Large-Eddy Simulation IV*. 2001, pp. 55–66.
[62] J. Wouters, S. Dolaptchiev, V. Lucarini, and U. Achatz, Parameterization of stochastic multiscale triads. *Nonlinear Processes in Geophysics* **23** (2016), 435–445.
[63] J. Wouters and V. Lucarini, Disentangling multi-level systems: averaging, correlations and memory. *J. Stat. Mechanics: Theory and Experiment* **2012** (2012), No. 3, P03003.